EPSC Abstracts
Vol. 11, EPSC2017-855, 2017
European Planetary Science Congress 2017

Modelling the effects of gravity waves in the GEM-Mars GCM

L. Neary, F. Daerden and S. Viscardy
Royal Belgian Institute for Space Aeronomy, Brussels, Belgium (lori.neary@aeronomie.be)

Abstract

Parameterizations for orographic and non-orographic gravity waves are included in the GEM-Mars general circulation model (GCM) for low-resolution simulations. The impacts of these parameterizations on the temperature and winds in the upper atmosphere are examined and sensitivity studies are discussed.

1. Introduction

Gravity waves have been observed in the Martian atmosphere (e.g. Creasey et al., 2006, England et al., 2017) and are considered to have an important impact on the temperature and dynamics of the upper atmosphere.

The waves can be produced by flow over topography and propagate upwards to break in the upper atmosphere. This has the effect of depositing energy and momentum into the mean flow, altering the general circulation patterns. Other sources of gravity waves include wind shears and instabilities (called non-orographic). As it is computationally expensive and impractical to run a GCM at a horizontal resolution high enough to resolve gravity waves, it is necessary to parameterize their effects on the grid-scale winds in the model.

For Earth, it has been shown that the inclusion of a parameterization for both orographic and non-orographic wave drag in climate models is necessary to properly reproduce the extratropical stratospheric/mesospheric circulation. It has become increasingly accepted that the effects of these types of waves should also be included in Martian GCMs.

Here we evaluate the results of simulations made with the GEM-Mars GCM (Neary and Daerden, 2017) including parameterizations for both orographic and non-orographic gravity wave drag. A comparison of temperatures with those observed by the Mars Climate Sounder (MCS) (McCleese et al., 2007; Kleinböhl et al., 2009) help to assess the impact of these schemes.

2. Methods

We use the GEM-Mars GCM at a horizontal resolution of 4°×4° with 103 vertical levels up to a height of ~150 km to test the parameterizations. A brief description of the model is given here, as well as a description of the experiments performed.

1.1 Model description

GEM-Mars is grid-point model with a semi-Lagrangian advection scheme and a two-time-level semi-implicit integration method. For the 4°×4° horizontal resolution presented here, we use an integration time step of 1/48th of a Martian sol.

The model simulates interactive carbon dioxide-, dust-, water- and atmospheric chemistry cycles. Dust and water ice clouds are radiatively active. Size distributed dust is lifted by saltation and dust devils. The model includes 16 chemical species and has fully interactive photochemistry and gas-phase chemistry.

For the effects of orographic gravity wave drag, we use the scheme described by McFarlane (1987). The sub-grid scale parameters are derived from the high resolution MOLA topography. A low-level blocking scheme is also incorporated (Zadra et al., 2003). The gravity wave drag (GWD) scheme relies on the saturation concept of Lindzen (1981) to calculate the vertical structure of the wave drag force. The changes in the horizontal wind due to GWD depend on the sub-grid scale orographic variance, the atmospheric stratification, local density height scale and a tunable parameter defined as the product of a representative value of horizontal wavenumber and an efficiency factor less than one. For Mars, this parameter was reduced from the terrestrial value. In the wave

saturation regions, the wave amplitude is set according to a critical Froude number that is set to $\sqrt{0.5}$. This number is also considered a tuning parameter, but kept unchanged here.

For the effects of non-orographic gravity waves, we use the scheme of Hines (1997a,b). This method uses the Doppler-spread theory of gravity wave saturation where breaking is represented by imposing an upper limit to the range of vertical wavenumbers in the spectrum that can propagate above some altitude considered. The wavenumber upper limit at some azimuth j at a given altitude is given by:

$$m_j = \frac{N_0}{\Phi_1 \hat{\sigma}_j + \Phi_2 \hat{\sigma}_h + V_j - V_{0j}}$$

where N_0 is the buoyancy frequency at the source level, $\hat{\sigma}_j$ is the gravity wave wind standard deviation in direction j at altitude z, $\hat{\sigma}_h$ is the total gravity wave wind standard deviation at altitude z, V_j is the background wind in direction j at the source altitude and Φ_1 and Φ_2 are tunable parameters.

1.2 Scenarios/Experiments

Comparisons are made between simulations performed with orographic GWD only and with both orographic and non-orographic GWD.

There are several parameters to be set in the non-orographic GWD scheme. The initial simulation shown here uses a source level of ~10 km, 8 equally spaced azimuths, Φ_1 = 1.5, Φ_2 = 0.3, an equivalent horizontal wavenumber k^*, which represents the mean horizontal wavelength of the gravity wave spectrum of 200 km and a lower bound vertical wavenumber m_{min} which imposes a limit on the allowable maximum vertical wavelength of 12 km. For the orographic GWD scheme, we use a value 5×10^{-6} for the tunable parameter.

3. Results

The top row of Figure 1 shows the difference in zonal mean temperatures between the two simulations for the two equinox seasons. In the winter pole between 1 and 0.01 Pa, there is a cooling effect, on the order of ~20 K. Compared with MCS, the run with non-orographic GWD (bottom row in Figure 1) reduces the warm bias seen in the run with orographic GWD only (2nd row in Figure 1). The results are encouraging, but further tests are required to examine the sensitivity to parameters in both parameterizations.

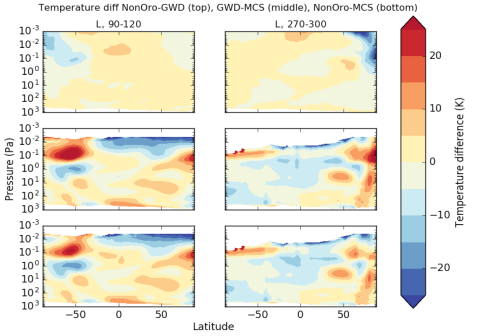

Figure 1 Temperature differences between 2 model simulations and MCS observations for 2 seasons: Left column is northern summer solstice (L_s=90-120°), right column is northern winter solstice (L_s=270-300°). The top row is the difference between the run with both orographic and non-orographic GWD (NonOro) and with orographic only (GWD). Middle row is NonOro-MCS, bottom row is GWD-MCS.

4. Summary and Conclusions

Initial tests with the non-orographic GWD parameterization included in GEM-Mars indicate that the strongest effects on temperature are seen in the solstice periods at L_s = 90° and 270° in the upper atmosphere of the winter polar region. Between 1 and 0.01 Pa, a cooling on the order of 20 K is seen in the winter pole, giving better agreement with MCS temperatures. There is little change during the equinox periods (not shown here).

As GEM-Mars has the capability of running at a much higher resolution, it is possible to make a reference simulation where gravity waves are resolved to help quantify their effects and constrain the values used in the parameterizations.

Acknowledgements

This work received funding from the ESA PRODEX Office under the Exo-Mars NOMAD project.

References

Creasey, J.E., Forbes, J.M., Hinson, D.P., 2006. Global and seasonal distribution of gravity wave activity in Mars' lower atmosphere derived from MGS radio occultation data. Geophysical Research Letters 33. doi:10.1029/2005GL024037

England, S.L., Liu, G., Yiğit, E., Mahaffy, P.R., Elrod, M., Benna, M., Nakagawa, H., Terada, N., Jakosky, B., 2017. MAVEN NGIMS observations of atmospheric gravity waves in the Martian thermosphere: Gravity Wave Observations at Mars. Journal of Geophysical Research: Space Physics. doi:10.1002/2016JA023475

Hines, C., 1997a. Doppler-spread parameterization of gravity-wave momentum deposition in the middle atmosphere. Part 1: Basic formulation. Journal of Atmospheric and Solar-Terrestrial Physics 59.

Hines, C.O., 1997b. Doppler-spread parameterization of gravity-wave momentum deposition in the middle atmosphere. Part 2: Broad and quasi monochromatic spectra, and implementation. Journal of Atmospheric and Solar-Terrestrial Physics 59, 387–400.

Kleinböhl, A., Schofield, J.T., Kass, D.M., Abdou, W.A., Backus, C.R., Sen, B., Shirley, J.H., Lawson, W.G., Richardson, M.I., Taylor, F.W., Teanby, N.A., McCleese, D.J., 2009. Mars Climate Sounder limb profile retrieval of atmospheric temperature, pressure, and dust and water ice opacity. Journal of Geophysical Research 114. doi:10.1029/2009JE003358

Lindzen, R.S., 1981. Turbulence and stress owing to gravity wave and tidal breakdown. J. Geophys. Res 86, 9707–9714. doi:10.1029/JC086iC10p09707

McCleese, D.J., Schofield, J.T., Taylor, F.W., Calcutt, S.B., Foote, M.C., Kass, D.M., Leovy, C.B., Paige, D.A., Read, P.L., Zurek, R.W., 2007. Mars Climate Sounder: An investigation of thermal and water vapor structure, dust and condensate distributions in the atmosphere, and energy balance of the polar regions. Journal of Geophysical Research 112. doi:10.1029/2006JE002790

McFarlane, N.A., 1987. The effect of orographically excited gravity wave drag on the general circulation of the lower stratosphere and troposphere. Journal of the Atmospheric Sciences 44, 1775–1800.

Neary, L. and Daerden, F., 2017. The Gem-Mars General Circulation Model for Mars: Description and Evaluation, Icarus (in review).

Zadra, A., Roch, M., Laroche, S., Charron, M., 2003. The subgrid-scale orographic blocking parametrization of the GEM Model. Atmosphere-Ocean 41, 155–170. doi:10.3137/ao.410204